

## CHAPTER 4

---

---

# Highly Sensitive and Selective Room Temperature Operated NO<sub>2</sub> Sensor Based on Eco-friendly Water Processed Low Voltage Operable OFET.

---

---

Part of this work has been published as Prashant Kumar, V. N. Mishra, and R. Prakash, “Highly Sensitive and Selective Room Temperature-Operated NO<sub>2</sub> Sensor Based on Eco-Friendly Water Processed Low Voltage Operable OFET,” *IEEE Sens. J.*, vol. 23, no. 12, pp. 12544–12551, 2023, DOI: 10.1109/JSEN.2023.3271598.



---

## CHAPTER 4

---

---

### **Highly Sensitive and Selective Room Temperature Operated NO<sub>2</sub> Sensor Based on Eco-friendly Water Processed Low Voltage Operable OFET**

---

#### **4.1 Introduction**

Being one of the most toxic gas Nitrogen dioxide can result in permanent damage to the respiratory and cardiovascular systems in humans. Long-term exposure to NO<sub>2</sub> with a concentration as low as 1 ppm can result in respiratory system impairment and cardiovascular damage. People with a history of Asthma experience pulmonary impairment at NO<sub>2</sub> concentrations as low as 200 ppb. In addition to this, NO<sub>2</sub> also results in acid rain. Thermal power generation, vehicular exhausts, and metal refining centers constitute primary sources of NO<sub>2</sub>. Additionally, NO<sub>2</sub> is used as a biomarker for gastrointestinal illness symptoms and lung infection symptoms in medical diagnostic procedures[102]–[106]. The development of highly selective NO<sub>2</sub> gas sensors with low detection limits is essential for uses like environmental and health monitoring. Besides that, its low voltage and room temperature operation are essential for integration into Internet-of-Things (IoT) sensor nodes and continuous monitoring of air quality and health [54], [102]–[105]. Many gas sensors for sensing poisonous gases based on electrochemical sensing, optical sensing, surface wave sensing, and OFET (organic field effect transistor) based sensors[54], [102], [114], [103], [107]–[113] have been explored over the year. However, the OFETs based gas sensors are gaining popularity because of its advantage of the ease of fabrication, low processing cost, superior sensitivity, and multi-parameter

monitoring options like threshold voltage, drain current, mobility variation, and subthreshold swing for sensing. Nonetheless, OFET-based sensors generally require a high voltage of operation which makes it difficult to integrate them with portable monitoring systems[54], [102]–[105]. High  $k$  dielectrics like AlO<sub>x</sub>, ZrO<sub>x</sub>, HfO<sub>x</sub> has been commonly used to reduce the operation voltage of OFETs[98], [115]. In comparison with other organic solvents for solution processed dielectrics, water is regarded as the most eco-friendly solvent. Moreover water-induced processing is comparatively low cost and eco-friendly with respect to toxic organic solvents like ethylene glycol and 2 methoxy ethanol[36].

FTM (floating film transfer method) technique (in which floating film is lifted from the surface of organic or water substrate) is suitable for large area processing and has minimal wastage of costly organic semiconductor material (OSC), no need for sophisticated instruments, good film thickness control, and suitability for flexible devices, in the past when used with other polymers has shown to have superior gas sensing performance with respect to spin coating process[47], [77], [78]. Since charge transfer in OFETs actually occurs within a few layers of monolayer thickness near the dielectric interface, high-quality thin films obtained through FTM, are well suited for gas sensing applications. Consequently, thinner FTM films ensure the maximum interaction with gas molecules. [77].

Poly[2,5-(2-octyldodecyl)-3,6-diketopyrrolopyrrole-alt-5,5-(2,5di(thien-2-yl)thieno [3,2-b]-thiophene)] abbreviated as DPP-DTT has been used for NO<sub>x</sub> sensing in past using breath figure molding however the process is complex and requires costly equipment like a glove box and strict humidity control[54]. To the best of our knowledge, the FTM-transferred DPP-DTT film has not been tested for NO<sub>2</sub> sensing. In this paper, we have combined the advantages of eco-friendly processing of dielectric (Aluminum oxide) using Deionized (DI) water for low voltage

OFET operation[94] and superior gas sensing properties of the Floating film transfer method which again used water as a liquid substrate for self-assembled film transfer of DPP-DTT, whereas most of the gas sensors using FTM film [44], [77], [78], [114], [116], [117] have used Ethylene Glycol and Glycerol as a liquid substrate which is toxic to human health and the environment. In summary this chapter presents a highly selective and ppb level NO<sub>2</sub> sensor utilizing water processed AlO<sub>x</sub> dielectric based low voltage operable OFET. The semiconducting layer of ultra-thin DPP-DTT has been transferred using large area suitable W-FTM method. A comprehensive change in various characteristics such as mobility, threshold voltage, subthreshold swing, and trap density variation has been evaluated in relation to changes in different gas concentrations. A selectivity investigation with different other gases was carried out. Apart from this effect of humidity has also been studied. Finally, a mechanism of enhancement has been discussed. This chapter is divided into six sections including this. The section 4.2 covers steps involved in device fabrication followed by section 4.3 which covers surface morphologies of the transferred film of DPP-DTT. The section 4.4 discusses the electrical and gas sensing characteristics of the fabricated device followed by section 4.5 which presents the obtained result with discussion and comparison. Finally, section 4.6 concludes the findings of the chapter.

## **4.2 Device Fabrication**

**Materials Details:** DPP-DTT (poly[2,5-(2-octyldodecyl)-3,6-diketopyrrolopyrrole-alt-5,5-(2,5di(thien-2-yl) thieno [3,2-b]-thiophene)]) (Mw. = 10200) was procured from Ossila Ltd UK. Aluminum nitrate hexahydrate and chloroform were purchased from Sigma Aldrich.

Firstly, p type <100> silicon substrate with a resistivity of 0.01- 0.02 Ω-cm was diced into a

specific size of 2 cm x 1.5 cm and cleaned using isopropanol, acetone, and methanol in an ultrasonic setup for 15 min each and thoroughly rinsed using Deionized (DI) water. These diced and cleaned samples were then dried under a nitrogen environment. 0.3M Aluminum nitrate hexahydrate was dissolved in DI water over a magnetic stirrer for 12 hours and filtered through a 0.22  $\mu\text{m}$  syringe filter to remove undissolved larger particles. The freshly prepared 0.3M Aluminum nitrate solution was spin-coated on the silicon substrate (plasma cleaned for better adhesion) at 3000 rpm for 30 sec and then heated for 100°C for 15 min before being baked at 260°C for 2 hours. 3.5 mg/ml DPP-DTT was dissolved in a mixture of chloroform and 1,2 Dichlorobenzene using a magnetic stirrer for 6 hours. Then  $\sim 10 \mu\text{L}$  of the dissolved DPP-DTT was gently dropped over the still surface of DI water in a Petridis as shown in Fig. 4.1 (a) to form a self-assembled film of DPP-DTT. The self-assembled film of DPP-DTT was stamped onto the  $\text{AlO}_x$  coated substrate followed by heating for 30 min at 150°C. Then using the Hind Hivac 12A4D thermal evaporator and the Ossila interdigitated masks ( $W/L=18.23 \text{ mm} / 50 \mu\text{m} = 360$ , where W and L represent the width and length dimensions of the channel) gold electrodes were deposited at the vacuum of  $1.2 \times 10^{-6}$  Torr at 0.02 nm/sec. The schematic of the  $\text{AlO}_x/\text{DPP-DTT}$  OFET with Interdigitated electrode is shown in fig. 4.1(b).

### 4.3 Surface Morphologies

Surface morphologies of water-processed  $\text{AlO}_x$  film and DPP-DTT film stamped from water surface were studied using NTEGRA Prima Scanning probe microscope in tapping mode as shown in Fig. 4.2 (a) and b) respectively. The root mean square (rms) roughness of water-processed  $\text{AlO}_x$  film was  $\sim 0.164 \text{ nm}$ . The sensing film of FTM transferred DPP-DTT has rms roughness ( $s_q$ ), average roughness ( $s_a$ ), area peak to valley height ( $s_t$ ), maximum area peak

height ( $s_p$ ), and maximum area valley depth ( $s_v$ ) of 3.115 nm, 2.459 nm, 31.558 nm, 18.253 nm, and 13.304 nm respectively. The film thickness of DPP-DTT film was measured using Filmetrics FV 20 UV and was found to be  $12 \pm 2$  nm. Such nanometer roughness and low film thickness are suitable for superior gas sensing properties [44], [77]–[79], [114], [116], [117].

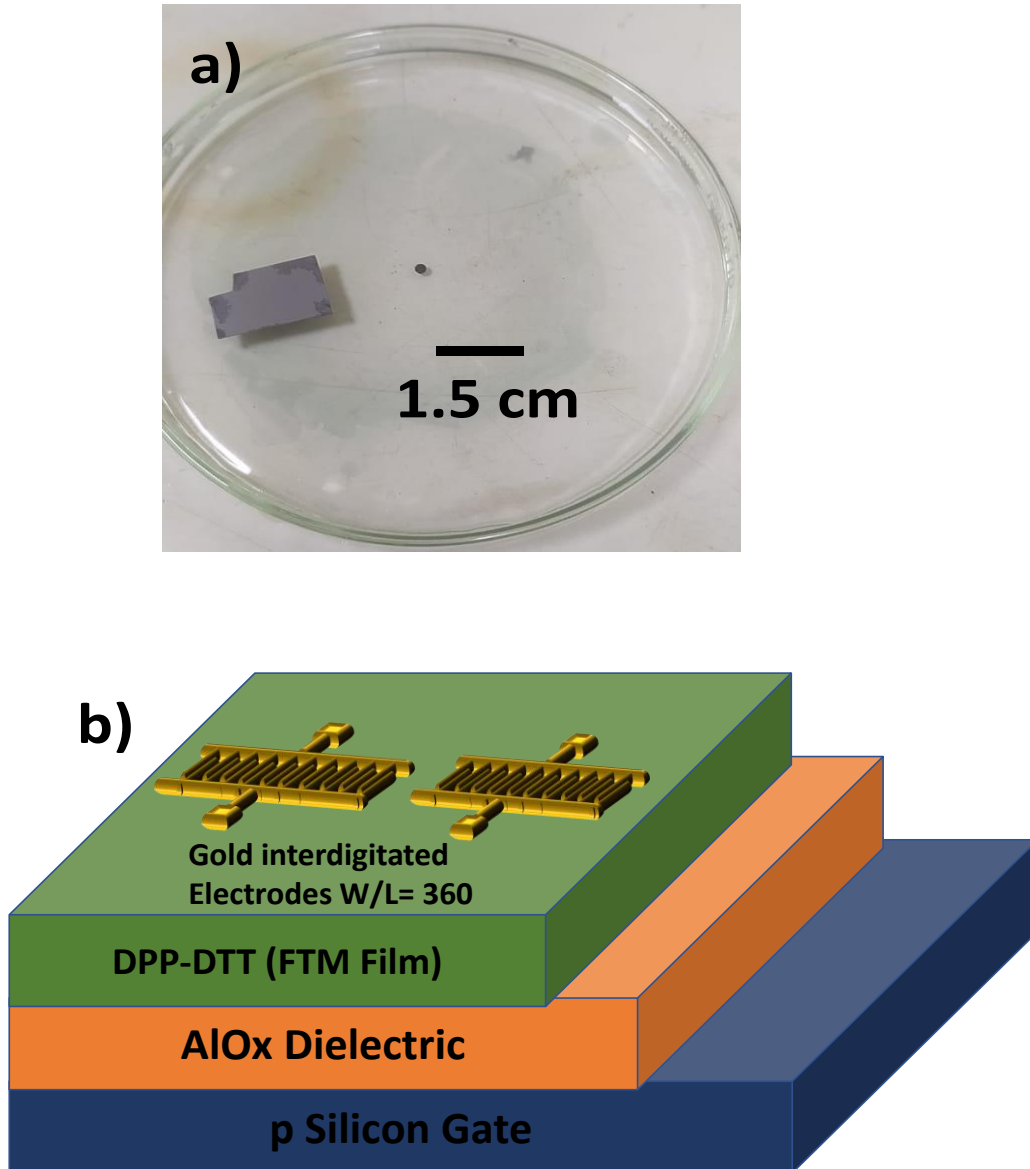


Fig.4.1 (a) Floating film of DPP-DTT on water surface b) schematic of the DPP-DTT/AIO<sub>x</sub> OFET.

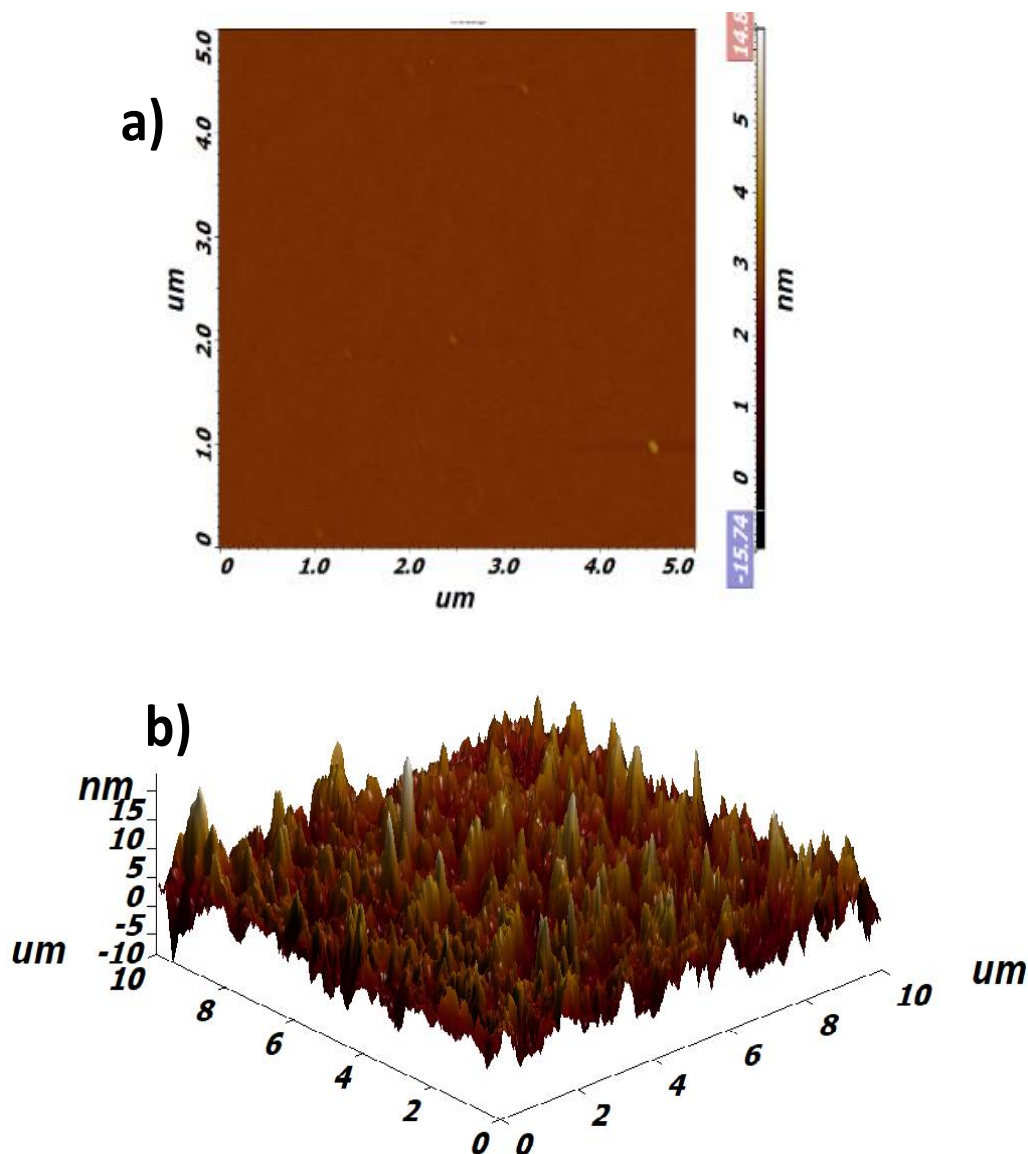


Fig. 4.2. (a) AFM image of AlO<sub>x</sub> film on the silicon substrate (b) AFM image of DPP-DTT FTM film.

## 4.4 ELECTRICAL AND GAS SENSING CHARACTERIZATION

### 4.4.1 ELECTRICAL CHARACTERIZATION

All Electrical measurements of the OFETs were carried out in the air using a Keysight B1500A semiconductor parameter analyzer on a specially designed probe station under 55% RH, and  $V_{DS} = -3$  V at 25°C. The respective output and transfer characteristics of DPP-DTT-based OFET, measured in open ambient, are shown in Fig. 4.3 (a) and (b). The threshold voltage

( $V_{TH}$ ) and saturation mobility ( $\mu_{sat}$ ) were extracted by using maximum slope (m) and intercept (C) of the linearly fitted square root of  $I_{DS}$  versus  $V_{GS}$  curve of the device as per the equation (4.1), (4.2), and (4.3)[44], [117].

$$I_{DS} = \frac{W\mu_{sat}C_{ox}}{L} (V_{GS} - V_{TH})^2 \quad (4.1)$$

$$\sqrt{I_{DS}} = \sqrt{\frac{W\mu_{sat}C_{ox}}{L}} (V_{GS} - V_{TH}) = Y = mX - C \quad (4.2)$$

$$Y = mX - C \quad (4.3)$$

The extracted value of saturation mobility ( $\mu_{sat}$ ) and threshold voltage ( $V_{TH}$ ) of the DPP-DTT device in the air was  $5.55 \times 10^{-3} \text{ cm}^2\text{V}^{-1}\text{S}^{-1}$  and -1.21 V respectively at  $V_{DS} = -3 \text{ V}$ . Subthreshold swing (SS) and trap density (TD) were calculated using the equation (4.4) and (4.5) respectively [44], [117] where q, c, k, and T represents charge, the capacitance of dielectric layer, Boltzmann constant, and temperature in kelvin respectively.

$$SS = \left( \frac{d I_{DS}}{d V_{GS}} \right)_{max}^{-1} \quad (4.4)$$

$$TD = \frac{c}{q} \left( \frac{qSS}{kT \ln 10} - 1 \right) \quad (4.5)$$

#### 4.4.2 Gas Sensing Charecterization

In order to evaluate gas sensing performance, we exposed the in-house designed test chamber

with varying concentrations of NO<sub>2</sub> starting from 200 ppb to 1.4 ppm and respective change in  $I_{DS}$  versus  $V_{GS}$  was recorded. A certain amount of NO<sub>2</sub> of 99.99% purity was taken out of the portable cylinder using an air tight syringe. The appropriate concentration of NO<sub>2</sub> was obtained using dilution through the ambient air. The experiment was repeated 5 times to check the repeatability. Since NO<sub>2</sub> is a strong oxidizing agent, the drain current increases due to an increase in hole carrier concentration. Fig. 4.4 (a), (b), and (c) represents the comparative  $I_{DS}$  versus  $V_{GS}$  curve, logarithmic  $I_{DS}$  vs  $V_{GS}$  curve, and the square root of  $I_{DS}$  versus  $V_{GS}$  after exposure to different concentrations of NO<sub>2</sub>.

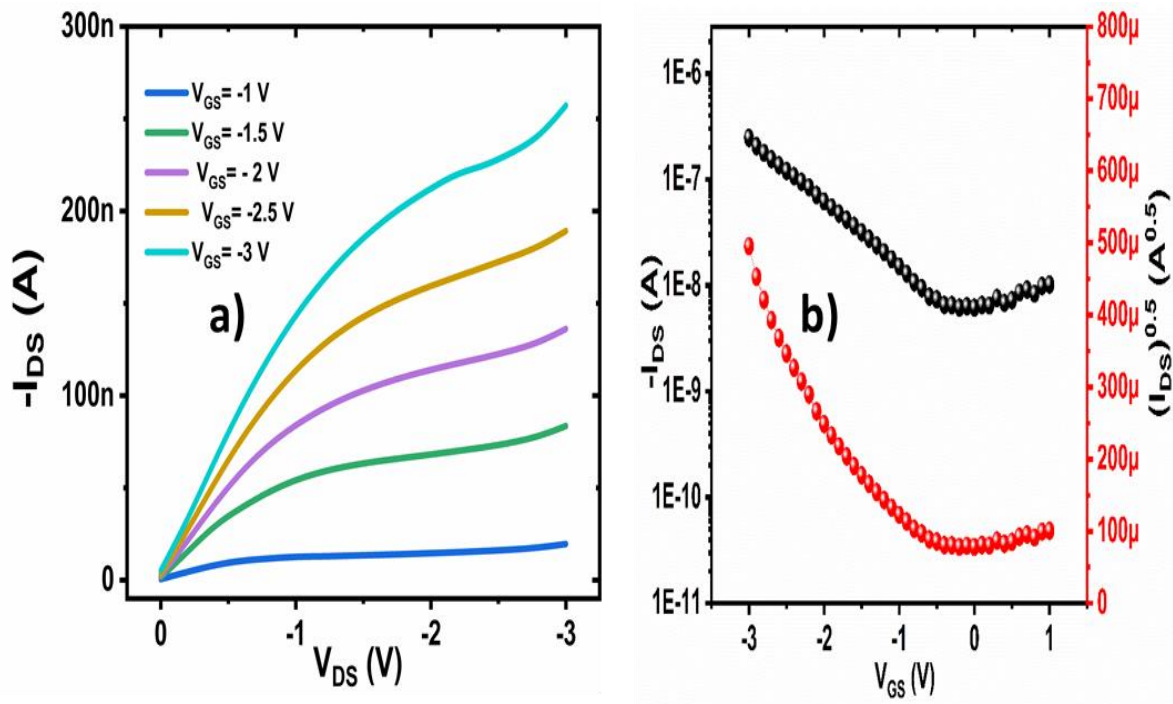


Fig.4.3. (a) Output characteristics (b) transfer characteristics of AlOx/DPP-DTT OFET at  $V_{DS} = -3$  V.

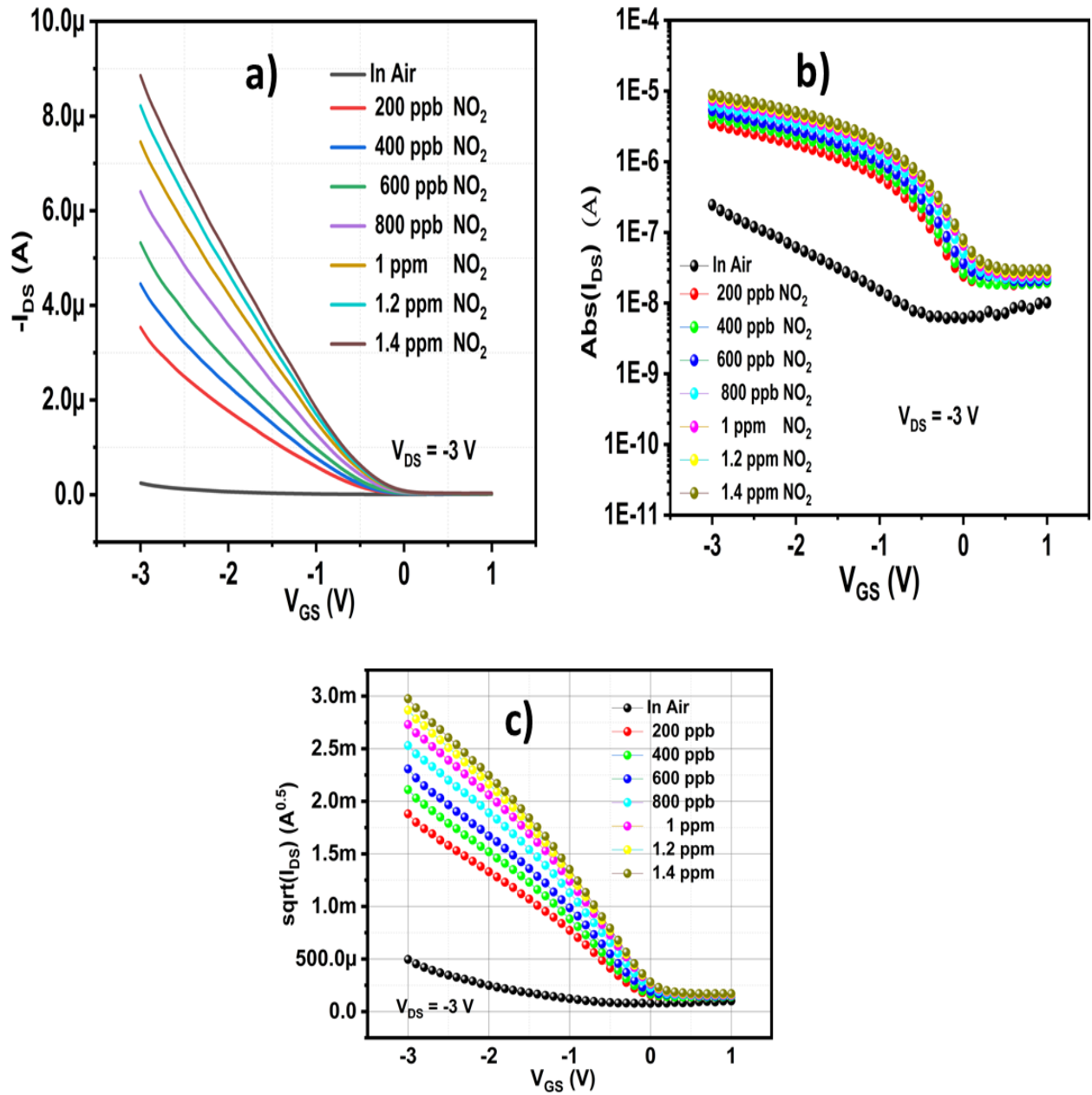


Fig. 4.4. (a) Transfer characteristics of AIO<sub>x</sub>/DPP-DTT OFET at  $V_{DS} = -3$  V (b) respective semi-logarithmic curve (c) respective square root of drain current curve in air and at different concentration of exposed Nitrogen dioxide.

## 4.5 Result and Discussion

### 4.5.1 Gas Sensing Response

Nitrogen Dioxide is a strong oxidizing gas that strongly withdraws electrons from the surface of polymer film thereby increasing the hole concentration which finally increases drain current, enhancement of mobility, and reduction in threshold voltage. The respective change in drain current called response (R) was calculated using the formula given by eq. (4.6) at  $V_{GS} = -1.5$  V and  $V_{DS} = -3$  V: where  $I_{DS,gas}$  and  $I_{DS,air}$  are drain currents after gas exposure and in ambient conditions respectively. Response percentage can be calculated by

$$R(\%) = \frac{|I_{DS,gas} - I_{DS,air}|}{I_{DS,air}} \times 100 \quad (4.6)$$

Percentage change in the drain current (R), summarized in Table 1, was observed to be 2217.4 % for 200 ppb and 8445.5 % for 1.4 ppm of NO<sub>2</sub> respectively. The percentage response (R) versus different concentrations of nitrogen dioxide has been plotted with its linear fit in Fig. 4.5 (a) while the linear fit of the response is depicted in Fig. 4.5 (e). For the calculation of the Limit of Detection (LOD) we have used the formula [44]:

$$LOD = \frac{3\sigma}{m} \quad (4.7) \quad ; \quad \frac{\mu_{gas} - \mu_{air}}{\mu_{air}} \times 100 \quad (4.8)$$

Where  $\sigma$  is the standard deviation and  $m$  is slope of the linear fit. The theoretical value of LOD was calculated to be  $16 \pm 4$  ppb. Since OFET-based gas sensing is a multi-parameter variation we have also calculated the percentage change in the mobility and threshold voltage with respect to the change in concentration of exposed nitrogen dioxide as shown in table 1. The respective change in mobility with concentration change was calculated using equation 4.8.

Table 4.1

SUMMARY OF MOBILITY AND THRESHOLD VOLTAGE CHANGES ON  
DIFFERENT CONCENTRATIONS OF NITROGEN DIOXIDE

<b>Mobility (<math>\mu</math>)</b> ( $\text{cm}^2\text{V}^{-1}\text{S}^{-1}$ ) $\times$ ( $10^{-3}$ ) <b>(Percentage</b> <b>change</b> ( $\frac{\mu_{gas}-\mu_{air}}{\mu_{air}} \times 100$ )	5.55 (0)	31.11 (460.54)	44.89 (708.82)	58.29 (950.27)	65.45 (1079.27)	67.15 (1109.90)	69.37 (1150)	72.87 (1210.81)
<b>Threshold</b> <b>Voltage</b> ( $\frac{V_{TH,gas}-V_{TH,air}}{V_{TH,air}} \times$ <b>100</b> )	-1.2 1 V	0.084 V (108.42)	0.122 V (110.41)	0.169 V (114.08)	0.203 V (116.98)	0.225 V (118.75)	0.244 V (120.33)	0.2628 V (121.92)
<b>Subthreshold</b> <b>Swing (SS)</b> (V/decade) ( $\frac{SS_{gas} - SS_{air}}{SS_{air}}$ $\times 100$ )	1.42 (0)	1.06 (-25.35)	0.855 (-39.78)	0.737 (-48.09)	0.55 (-61.12)	0.51 (-63.38)	0.49 (-65.54)	0.47 (-66.90)
<b>Trap charge</b> <b>density (TD)</b> ( $10^{12}$ )/ $\text{cm}^2$ (% change)	12.98 (0)	9.54 (-26.50)	7.59 (-41.52)	6.46 (-50.23)	4.67 (-64.02)	4.29 (-66.94)	4.10 (-68.41)	3.91 (-69.87)
<b>NO<sub>2</sub></b> <b>concentration</b> (ppm)	0	0.2	0.4	0.6	0.8	1	1.2	1.4

TABLE 4.2

SUMMARY OF PERCENTAGE RESPONSE (R) AT DIFFERENT  
CONCENTRATION

<b>Concentration of NO<sub>2</sub></b> <b>(ppm)</b>	<b>0.2</b>	<b>0.4</b>	<b>.6</b>	<b>0.8</b>	<b>1</b>	<b>1.2</b>	<b>1.4</b>
<b>% Response (R)</b>	2217.4	2983.3	3980.8	5690.6	7092.6	7829.9	8445.5

Upon exposure to 200 ppb and 1.4 ppm of NO<sub>2</sub>, the change in mobility was observed to be 460% and 1250% respectively. Whereas the threshold voltage change was found to be

108.42% and 121.92% for 200 ppb and 1.4 ppm of NO<sub>2</sub>. Mobility and threshold voltage changes for different concentrations of Nitrogen dioxide have been summarized in table 1 while Fig. 4.5 (b) and (c) depict the percentage change of mobility and threshold voltage respectively.

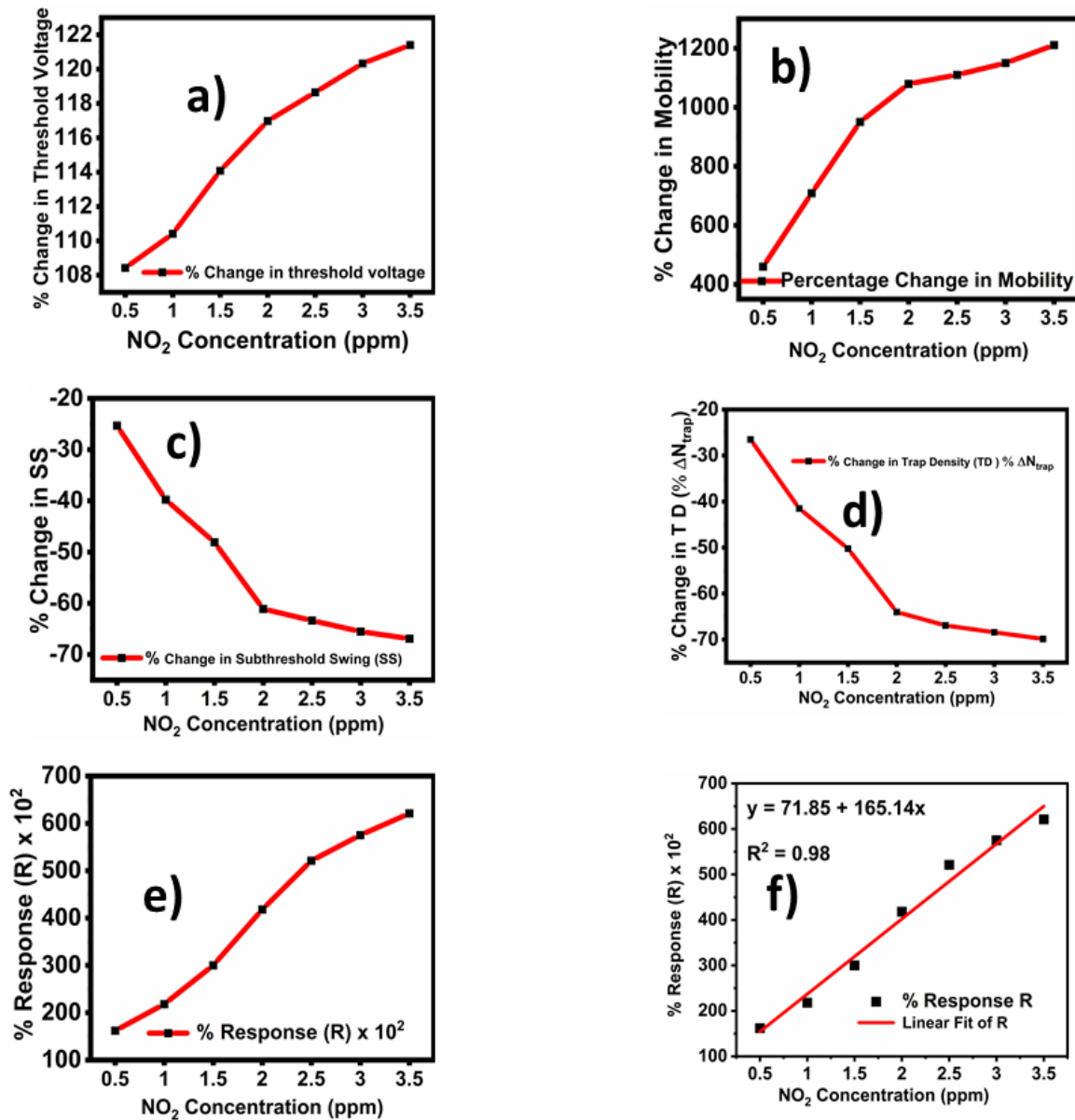


Fig. 4.5. (a) % change in threshold voltage (b) % change in mobility (c) % change in subthreshold swing (d) % change in trap density (TD) (e) % Response (f) linear fit of response ( $R^2 \sim 0.98$ ) at different concentrations of exposed nitrogen dioxide.

### 4.5.2 NO<sub>2</sub> Sensing Mechanism

Gas Sensing mechanism can be explained by taking into consideration the effect of the thin film obtained by FTM, the strong electron-withdrawing nature of NO<sub>2</sub>, and the significant surface roughness of ~ 3.115 nm as shown in Fig. 4.2 (b) thereby increasing the effective surface to volume ratio. A continuous and highly ordered organic semiconducting (OSC) layer is needed for the proper charge transport in OTFT, whereas for gas sensing, an extremely low thickness of the OSC layer is required to reduce the time of absorption/desorption of gas molecules [77], [114]. While in a thick film (Fig. 4.6 (b)), the molecules have to travel through (diffuse) practically the entire thick film of the OSC before they interact with the region near to dielectric-OSC interface where actual charge transfer occurs, adsorbed gas molecules on the thinner OSC surface start interacting directly with the charge carriers accumulated at OSC-dielectric interface. So, the diffusion path length of the gas molecule is reduced in thinner film (Fig. 4.6(a)) in comparison to thicker OSC films.

However, making a continuous and extremely thin film at the same time is a very difficult task and at the same time too much thinner film has the risk of electrode metal penetration at the time of deposition. We have optimized the concentration of DPP-DTT to get a continuous and thin film at the same time using FTM. Below 3.5 mg/ml the Floating film cracked over the water surface so the optimum concentration of 3.5 mg/ml was selected for this application.

The interacting gas molecule, generally, acts as either a dopant or trap center for the normal charge carriers in the polymer film. This can further be explained using trap density calculations. On exposure to NO<sub>2</sub>, there is a drastic reduction in trap density as shown in Fig. 4.5 (d). This is because due to exposure of NO<sub>2</sub> molecules the deep traps are filled thereby

reducing trap density and reducing the probability of trapping holes injected by the gate electrode. The same is illustrated by a decrease in subthreshold swing and an increase in mobility on exposure to NO<sub>2</sub> as shown in Fig. 4.5 (c). Such high response (R) can be attributed to three factors namely significant Dipole moment of donor-acceptor polymer DPP-DTT, and the role of thin film (of few monolayers) in gas sensing as discussed above. In contrast to homopolymers, donor-acceptor polymers like DPP-DTT have a substantially higher dipole moment for their repeating units [1]. NO<sub>2</sub>, being oxidizing gas and because of its strong electron-withdrawing property (as shown in Fig. 4.6 (c)), interacts significantly with the DPP-DTT molecule via dipole-dipole interaction through donor-acceptor groups of the polymer.

### **4.5.3 Effect of Humidity on DPP-DTT based NO<sub>2</sub> Sensor**

A gas sensor must perform satisfactorily under changing humidity conditions. In order to test the effect of humidity on the sensing performance of the DPP-DTT based NO<sub>2</sub> sensor, we measured the response of the sensor at different percentages of humidity for 200 ppb and 1000 ppb of NO<sub>2</sub>. The humidity was varied by injecting water vapor into the test chamber and measuring it through a humidity meter. This ensured effective control of % relative humidity of the chamber. As depicted in Fig. 4.7 (a) and (b), there is a slight increase in response (R). This may be attributed to the formation of HNO<sub>3</sub> in the presence of water vapor due to reaction with exposed NO<sub>2</sub>[118].

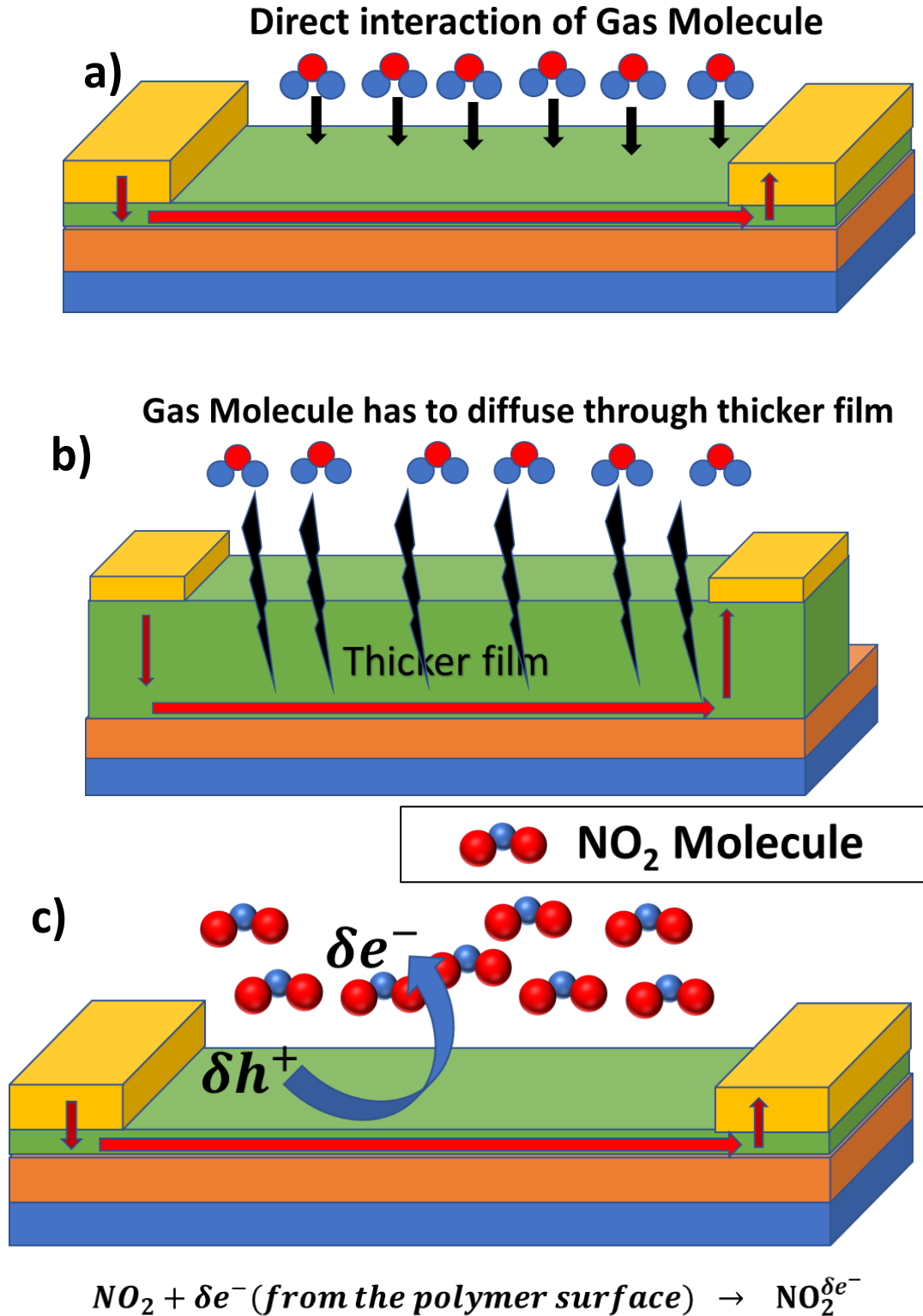


Fig.4.6. (a) Interaction of Gas Molecule with Thin film (b) Thick Film (c) and Electron Withdrawing phenomenon of Nitrogen dioxide.

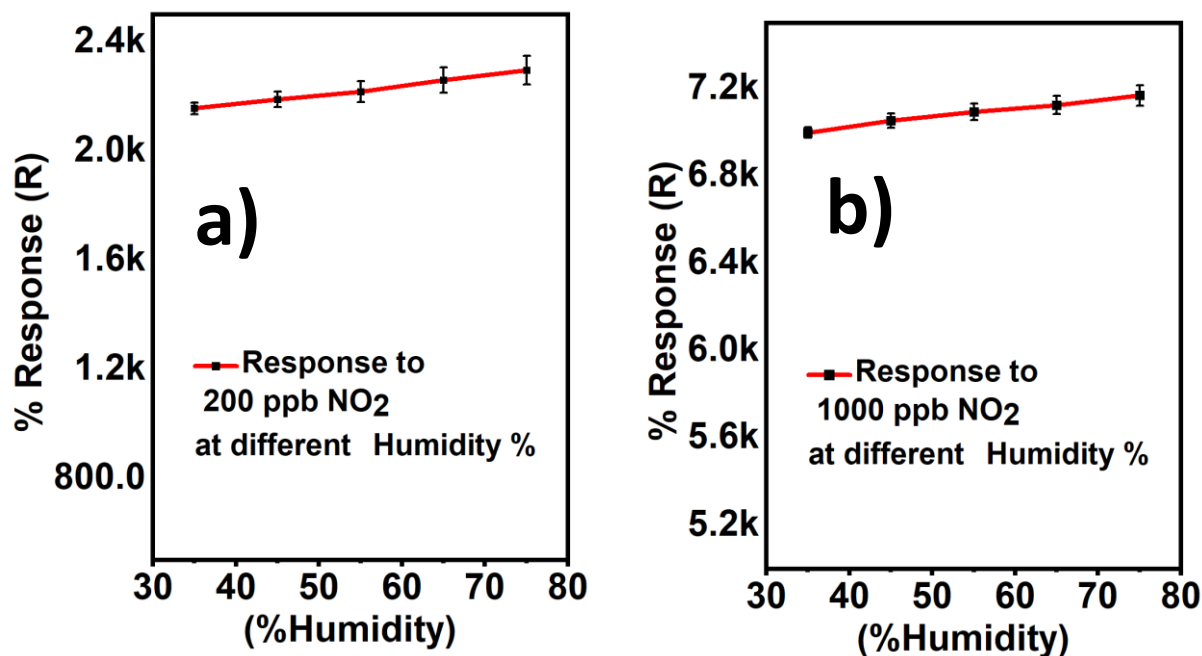


Fig. 4.7. (a), (b) Response to 200 ppb and 1000 ppb Nitrogen dioxide at different humidity percentage.

#### 4.5.4 Selectivity Study of DPP-DTT based NO<sub>2</sub> Sensor

A sensor must be selective to the target gas for which it has been designed. To test selectivity, we exposed the DPP-DTT-based OFET to various concentrations of gases like Sulphur dioxide (SO<sub>2</sub>), ammonia (NH<sub>3</sub>), hydrogen Sulphide (H<sub>2</sub>S) carbon dioxide (CO<sub>2</sub>), and H<sub>2</sub> gas. The respective percentage response (R) for different ppm of these gases is shown in Fig. 4.8. The Sulphur dioxide, being a weak oxidizing agent shows just a 178.6% change at 10 ppm concentration. Ammonia (NH<sub>3</sub>) and H<sub>2</sub>S show a negative response of 42.8% and 32.4% for 10 ppm concentration respectively while H<sub>2</sub> and CO<sub>2</sub> show a very feeble response at 50 ppm. Thus, the fabricated OFET-based sensor is highly selective to NO<sub>2</sub>.

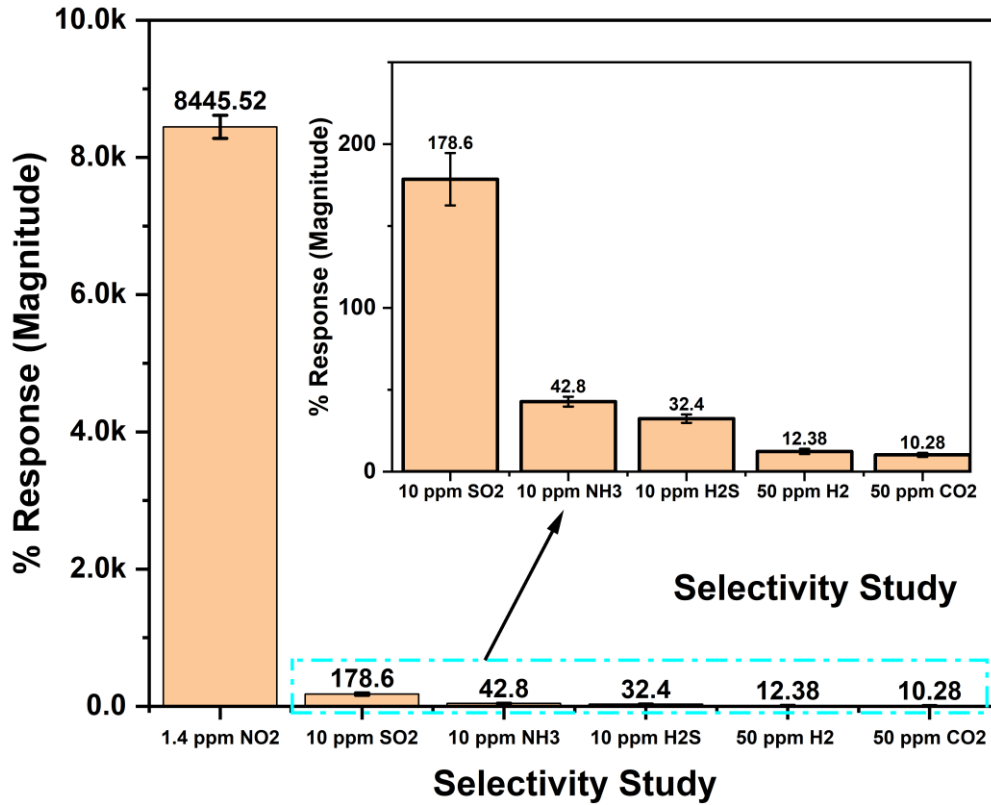


Fig. 4.8. Selectivity Study of AlO<sub>x</sub>/DPP-DTT OFET.

#### 4.5.5 Response time analysis of DPP-DTT NO<sub>2</sub> Sensor

The time it takes to respond to the gas analytes to reach 90% of the saturated response from 10% of the same when gas is turned on, is called rise time ( $t_r$ ), and then return from 90% to 10% of the saturated response after the gas is turned off is called fall time ( $t_f$ ). The rise and fall time for different concentrations of NO<sub>2</sub> has been studied as shown in Fig. 4.9. The rise and fall time for 200 ppb of NO<sub>2</sub> was recorded as 55 s and 104 s while it was 34 s and 176 s for 1 ppm.

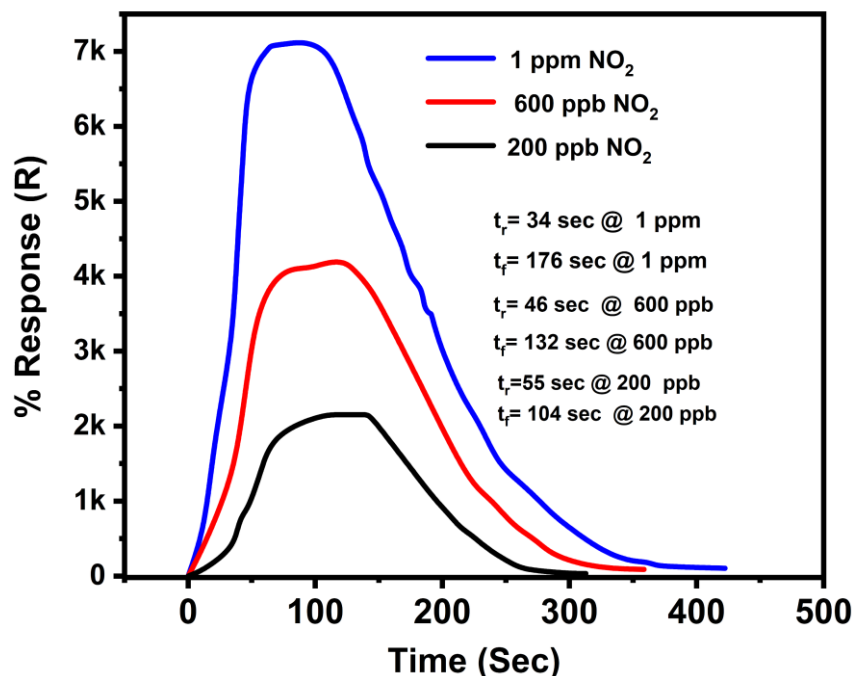


Fig. 4.9. Response time analysis of DPP-DTT OFET Sensor for Different concentrations of Nitrogen Dioxide.

#### 4.5.6 Comparative Study of DPP-DTT based NO<sub>2</sub> Sensor

In table 3 we have compared the reported OFET-based and other configurations of NO<sub>2</sub> sensors on various parameters like low voltage operability, room temperature sensing, response and recovery time, and low-cost fabrication. As only 10  $\mu\text{L}$  of DPP-DTT solution can create a film of  $\sim 10\text{ cm}^2$  over the surface of water (as can be seen in Fig. 4.1(a)), multiple films over different substrates or a single big substrate can be lifted, thereby making it a large area suitable and low-cost processing with minimal wastage of OSC material. Since we have used AlO<sub>x</sub> as a dielectric, it has ensured low voltage operation of the OFET device and hence low voltage sensing. The Breath Figure Moulding technique used in [54] requires a glove box and strict humidity control for the processing of the OSC layer, thereby making it costly, difficult to process, and unsuitable for large area processing. The thermal deposition method employed in

**TABLE 4.3 COMPARISON OF THE FABRICATED DEVICE WITH REPORTED NITROGEN DIOXIDE SENSORS**

Configuration	Material Used	Processing Technology	Voltage of Operation (V)	Response $\left(\frac{I_{DS,gas}-I_{DS,air}}{I_{DS,air}}\right) \times 100$	Temperature of Operation (°C) RT = room temperature	Response and Recovery Time ( $t_r/t_f$ ) (sec)	Remarks [references]
OFET	DPP-DTT	Breath figure Molding Using Spin coating.	-30	40000 % at 10 ppm (4000%/ ppm)	RT	NA	High voltage operation, Slow fabrication Process, requirement of Costly Glove box, and strict humidity control of 50-80% unsuitable for Large area fabrication [54]
OFET	TIPS Pentacene	Thermal Deposition system	-40	3083% at 3 ppm	RT	180/400	High Voltage operation, costly fabrication method [103]
OFET	TIPS Pentacene	Off-center spin coating	-40	221.5% @ 30 ppm	RT	More than 400 sec @ 1ppm /full recover not studied	High Voltage operation, not suitable for large-area fabrication [102]
Chemiresistive	Tantalum Pentoxide Alloyed Indium Oxide Rod Arrays	LASER interference Photolithography	NA	76.1 @ 100 ppm	110	48/329	Costly Fabrication method, High temperature required for operation [105]
Chemiresistive	Indium Oxide Nano flowers Decorated with Graphite nanoflakes	Hydrothermal Route	NA	120 $\left(\frac{I_{Gas}}{I_{Air}}\right)$ @ 1 ppm	75	130/41 (Recovery done after heating at 160°C) @ 1 ppm	High-temperature operation [104]
This Work	DPP- DTT	Floating Film Transfer Method (FTM) stamped from water surface	V <sub>DS</sub> = -3 V <sub>GS</sub> = -1.5	8445.52 % @ 1.4 ppm (7092.5%/ppm)	RT (25)	34/176 @ 1 ppm	RT operation, Suitable for large area processing, Eco-friendly processing, Low voltage operation

[103] can keep precise control over the thickness of the film, but it is costly, requires a sophisticated instrument, and results in wastage of OSC. LASER interference photolithography, as utilised in [105], again needs sophisticated instruments and is unsuitable for large area processing. Moreover, due to metal oxide, this device is working at 110°C, which requires an additional heating element, thereby increasing the power requirement. Off-the-centre spin coating method (used in compared reports) require sophisticated instruments and is not suitable for large area film transfer of active material. Off-the-centre spin coating used in [1] again results in wastage of OSC material and is not suitable for large area processing.

## 4.6 Conclusion

In this report, we combine the advantages of eco-friendly processing of aluminum oxide (AlO<sub>x</sub>) dielectric and FTM film of DPP-DTT over the water substrate for highly sensitive NO<sub>2</sub> gas sensing application. The low voltage operable OFET-based NO<sub>2</sub> sensor shows a remarkable response (R) of 8445%, % mobility change of 1210, % threshold voltage change of 121.92, and 66.90% reduction in Subthreshold swing on exposure to 1.4 ppm of NO<sub>2</sub>. The device shows quick response and recovery time of 34 s and 176 s respectively at 1 ppm. The considerable dipole moment of the donor-acceptor polymer (DPP-DTT) in comparison to homo polymer and the FTM transferred thin film of few monolayers are primarily responsible for such high response. Since FTM is suitable for large-area processing without the need for sophisticated instruments this result can be used for large-area NO<sub>2</sub> sensor fabrication while minimizing the costly OSC wastage and thus lowering the processing cost.